

RESEARCH

Open Access



Frankincense essential oil nanoemulsion specifically induces lung cancer apoptosis and inhibits survival pathways

Ahmed A. Abd-Rabou^{1*} and Amr E. Edris^{2*}

*Correspondence:
ahmedchemia87@yahoo.com;
ae.edris@nrc.sci.eg

¹ Hormones Department,
Medicine and Clinical Studies
Research Institute, National
Research Center, B.O. Box 12622,
Dokki, Cairo, Egypt

² Aroma & Flavor Chemistry
Department, Food Industries
& Nutrition Institute, National
Research Center, B.O. Box 12622,
Dokki, Cairo, Egypt

Abstract

Background: The volatile fraction of frankincense (*Boswellia sacra*) oleogum was extracted, formulated in nanoemulsion and tested against lung cancer A549 cell line. First, the gum was hydro-distilled to isolate the volatile fraction (essential oil), which was analyzed via gas chromatography to identify its major volatile constituents. Then, the oil was formulated in two water-based nanoemulsions which differ from one another in the presence of propylene glycol (PG), which is used in the formulation step as a co-surfactant. The pure essential oil as well as its major volatile compound (α -pinene), its two nanoemulsions and a reference drug (Doxorubicin) were evaluated against lung cancer A549 cell lines and WI-38 normal lung cells. The evaluation included cytotoxicity (MTT and IC_{50}), apoptosis (flow cytometric analysis) in addition to genetic assessments for some intrinsic and extrinsic genes relevant to apoptosis and survival pathways.

Results: Chromatographic analysis of frankincense essential oil revealed that α -pinene is the major volatile compound which constituent about 60% of that oil. Emulsification of the oil using the low energy technique gave nanoemulsions having major intense particles population (85–90%) with z-average diameter below 20.0 nm. Frankincense oil nanoemulsion fabricated with (PG) showed the best cytotoxic activity toward lung cancer A549 cell compared to PG-free nanoemulsion, α -pinene and the reference drug doxorubicin, along different incubation periods. Flow cytometric analysis also indicated that PG-containing nanoemulsion can induce cancer cells toward apoptosis better than the other formula and the pure oils. The same nanoemulsion was found to upregulate the pro-apoptotic genes [DR5, FAAD, Caspase 8 (Cas8), p53, and Bax] and downregulate the anti-apoptotic and reoccurrence genes (Bcl-2, NF-kB, and STAT-3). Most importantly, the PG-containing nanoemulsion had the least cytotoxic effect on the normal WI-38 lung cells.

Conclusions: These results point out to the potentials of frankincense essential oil (rich in α -pinene) and its PG-nanoemulsion as a promising adjuvant from plant-source to potentiate the activity of the systematic anti-lung cancer drugs.

Keywords: Frankincense, Essential oil, Lung cancer, Nanoemulsion, Apoptosis, Genes expression, Reoccurrence inhibition



Background

Lung cancer accounts for about 13% of all new cancer cases in both sexes worldwide (Siegel et al. 2021). It is classified into two main histological groups including small cell lung carcinoma which represents 15% of all lung cancers, and non-small cell lung cancer which represent the rest 85% of all lung cancers (Suster and Mino-Kenudson 2020). The latter group is further divided into three sub-groups known as adenocarcinoma, squamous cell carcinoma and large cell carcinoma (Rodriguez-Canales et al. 2016).

The primary treatment of lung cancer depends on surgical treatment (Hoy et al. 2019). In addition, patients after surgery may undergo additional adjuvant treatments (Passiglia et al. 2021). That can include chemotherapy (Li et al. 2022), radiation therapy (Khalifa et al. 2021), immune therapy (Xue et al. 2022), hormone therapy (Titan et al. 2020), and targeted therapy (Tan et al. 2022).

Beside the previously mentioned systematic procedures which are adopted in lung cancer management, phytochemicals are also emerging as adjuvants that can complementary participate in the therapy regime (Nguyen et al. 2021; Singh et al. 2021; Bittoni et al. 2021). Phytochemicals are chemical compounds derived from plants which have been used, since early times in folk medicine. Nowadays, different plant-based anticancer drugs are commercialized in the pharmaceutical market including for instance vinorelbine, etoposide, paclitaxel and camptotecin (Huang et al. 2021; Omara et al. 2020). These drugs have natural identity, equal efficiency and lower side effect compared to synthetic drugs.

Frankincense oleogum resin is considered to be a promising source of phytochemicals with diverse medicinal properties (Kieliszek et al. 2020). The oleogum is an exudate obtained by tapping the trunks of some trees belong to genus *Boswellia*. The anticancer-active phytochemical principle of frankincense was identified as boswellic acids (Katrangunta et al. 2019). They are a family of pentacyclic terpenoid molecules found in the non-volatile fraction of frankincense. The family consist of six members which showed diverse medicinal activity against inflammations (Börner et al. 2021), Alzheimer's (Siddiqui et al. 2021), different types of cancer (Efferth and Oesch, 2020), including lung cancer (Lv et al. 2020).

Beside boswellic acids in the non-volatile fraction, frankincense also contains a volatile oil fraction (called essential oil) which constitute 5–15% of the oleogum (Mertens et al. 2009). Frankincense essential oil (FEO) from different species showed potentials for application as supportive therapy for cancer-related fatigue (Reis and Jones 2018). In addition, different studies reported the inhibitory activity of FEO against various types of cancer cells via different mechanistic pathways (Hakkim et al. 2020; Ren et al. 2018; Suhail et al. 2011).

Despite the diversity of the above-mentioned studies beside others in the same line who evaluated many essential oils (Yoo et al. 2020), we noticed that there is no conclusive work on FEO which is directed specifically against lung cancer.

The number of new lung cancer cases, fatalities, and disability-adjusted life years was rising over the world. For example, that number showed twofold rise in 2017 compared to 1990 (Deng et al. 2020). Therefore, the current study aims to conduct in vitro comprehensive investigation in this direction to shed more light on the activity of FEO as potential lung cancer suppressing phytochemical. The study will also evaluate the effect

of nanoemulsion formulation of FEO on its anticancer activity in terms of apoptosis and genetic regulations including those which control survival pathways. Nanoemulsions are used as delivery system due to its water-based nature which allow intravenous administration, better cytotoxicity, enhanced therapeutic properties, long circulation time in the blood, beside other therapeutic benefits (Wilson et al. 2022; Ceramella et al. 2021). That is due to their small particle size which is normally in the range of 100 nm. The common methods used for nanoemulsion formulation include the low energy (Edris 2021) and the high energy (Falleh et al. 2021) techniques. In the current work, the low energy technique is adopted due to its different advantages that are discussed in the previously mentioned reference.

Materials and methods

Materials

Frankincense oleogum (*Boswellia sacra*), grade “Hougari, Fig. 1” was purchased from the ‘Luban market’ which is located in the city of Salala, Dhofar region, Sultanate of Oman.

Cremophor® RH40 (PEG-40 hydrogenated castor oil) and propylene glycol (PG) were purchased from Sigma Aldrich, USA. Sunflower oil was obtained from the local market.

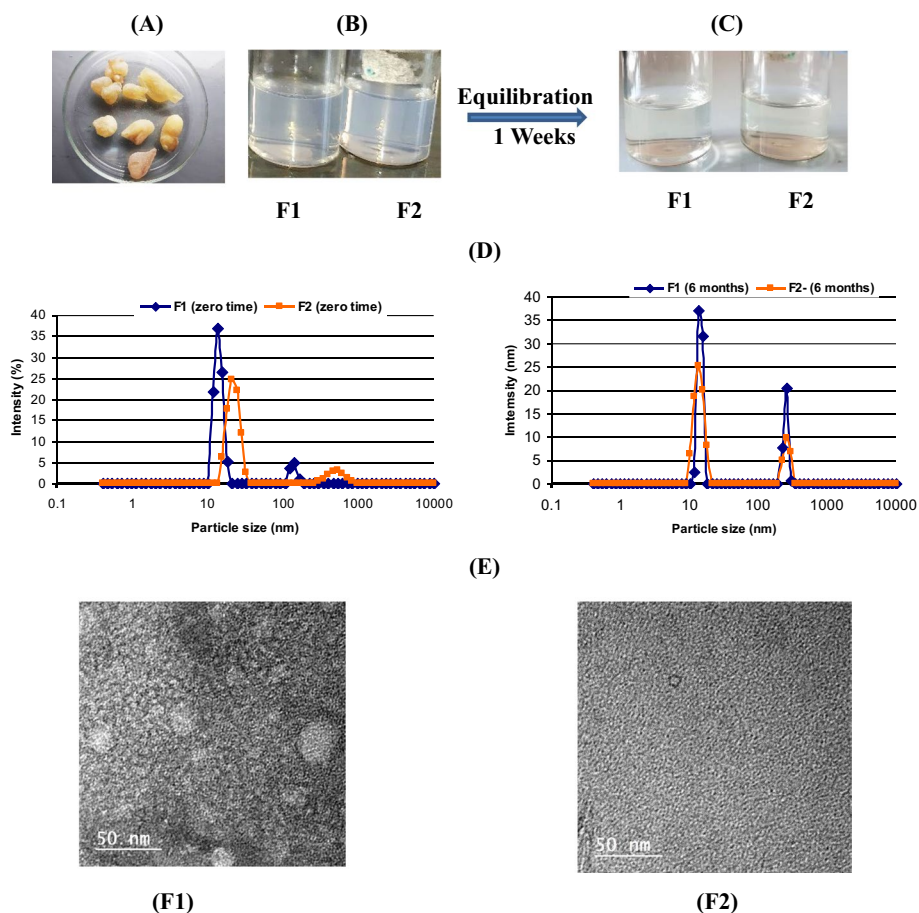


Fig. 1 A Frankincense oleogum; B, C appearance of frankincense essential oil nanoemulsions; D particle size distribution of nanoemulsions at zero time (left) and after 6 months storage period (right); E TEM photos of the nanoemulsions at zero time

The lung cancer A549 cell line and normal lung WI-38 cell lines were purchased from American Type Culture Collection (ATCC) supplied from VCSERA.

Isolation of FEO essential oil

The hydro-distillation technique was used to isolate the essential oil of frankincense. Different batches of frankincense gum (100 g each) were ground into fine powder and mixed (each) with 1000 ml of distilled water in 5L round bottom flask equipped with Clevenger-type apparatus. The gum powder and water were brought to boil for 2.5 h continuously using a heating mantle (Electrothermal EM 3000/CE). The vapors were condensed and the essential oil was collected as an upper layer from the side arm of the Clevenger apparatus at the end of distillation process. Finally, the collected oil was dried over anhydrous sodium sulfate, weighed and stored in dark glass vials at -4°C until analyzed.

Characterization of FEO volatile components

Gas chromatography (GC–FID) and gas chromatography–mass spectroscopic (GC–MS) analysis were used to separate and identify the major volatile constituents of FEO. The GC instrument equipped with flame ionization detector was Berkin Elmer Auto system XL, USA. For GC–MS analysis, Agilent model 8890 GC, 5977B GC/MSD system, USA was used. Details of the procedure including the conditions of analysis, the specification of the separating capillary column, along with the approaches of identification of the volatile compounds were fully described in our previous investigation (Abd-Rabou and Edris 2021).

Formulation of FEO nanoemulsions

Two FEO nanoemulsions denoted by (F1) and (F2) were formulated for the evaluation of their anti-lung cancer activity. Nanoemulsion F1 comprises FEO (5.0%), sunflower oil (1.0%), Cremophor RH40, (6.0%) and water (88.0%). Similarly, nanoemulsion F2 comprises FEO (5.0%), sunflower oil (1.0%) Cremophor RH40 (6.0%), water (87.0%) with an additional ingredient, namely, propylene glycol PG (1.0%), which was used as a co-surfactant.

The low energy emulsification technique was used for the formulation of both nanoemulsions. Briefly, all ingredients, except water, were mixed intimately in glass vials, then titrated into water with mild stirring using magnetic bar to give spontaneously FEO nanoemulsions. A detailed description of the emulsification process was indicated in our previous investigation (Abd-Rabou and Edris 2021).

Characterization of FEO nanoemulsions

Visual inspection

The samples of nanoemulsions were visually inspected by the naked eye against bright white light for detection of the general appearance regarding transparency and opalescence, which are a preliminary indication of the formation of nanoemulsion. The visual inspection was continued regularly during a storage period of 6 months.

Particle size analysis

The particle size of the nanoemulsions was measured, after equilibration period of 1 week at room temperature, using the dynamic light scattering instrument Zetasizer (Nano-ZS model ZEN3600, Nanoseries, Malvern Instruments, UK). Details of sample preparation and conditions of measurements were indicated in details in our previous relevant investigation (Abd-Rabou and Edris 2021).

Transmission electron microscopy (TEM)

Particle morphology of the formulated nanoemulsions was examined using TEM (Philips CM-10 FEI, In., Hillsboro, OR, USA). 50 μ l of each nanoemulsion was dropped into Formvar-coated copper grids and left to dry. Then, the samples were stained using 2% w/v uranyl acetate as a negative staining agent. Image capture and analysis were done using Digital Micrograph and Soft Imaging Viewer software (Electron Microscope Unite services), NRC, Egypt.

Physical stability

Samples of equal volumes (10 ml) of each of the freshly prepared nanoemulsions were placed in transparent screw-capped glass vials and left undisturbed upright on the bench at room temperature ($25\text{ }^{\circ}\text{C}\pm 2$) for 6 months. During this period, the samples were subjected regularly to visual inspection to observe any aspects of physical instability, such as oil separation or creaming. Particle size analysis was conducted one more time at the end of the storage period for more confirmation of the stability nanoemulsion particles.

Cancer cell cultivation

Lung cancer A549 cell line and normal lung WI-38 cell lines were cultivated in RPMI 1640 medium (Gibco) supplemented with 10% heat-inactivated fetal bovine serum (Gibco), 100 U/ml streptomycin, and 100 U/ml penicillin (Gibco) at $37\text{ }^{\circ}\text{C}$ in a humidified 5% CO_2 atmosphere.

Cell proliferation assay

All formulations were evaluated by MTT cytotoxic assay (van Meerloo et al. 2011) using lung cancer A549 cells and normal lung WI-38 cells. The cells were seeded in 96-well plates at a density of 1×10^4 cells/well and incubated for 4 h, 24 h, 48 h, and 72 h. Then, the cells were subsequently treated with 0, 20, 40, 60, 80, and 100 $\mu\text{g/ml}$ of FEO (denoted as F0), FEO nanoemulsions (F1, F2), α -pinene (denoted as PIN), and the reference drug Doxorubicin (denoted as DOX). On the other hand, control cells were treated with PBS which was incorporated in medium. After that, the cells were incubated with 1 mg/ml of MTT reagent at $37\text{ }^{\circ}\text{C}$ for 4 h, and then, it was discarded. The formed formazan crystals were dissolved using 100 μl of DMSO, followed by incubation and shaking. Finally, colorimetric analysis using a multiplate reader was measured at absorbance $A_{540\text{ nm}}$. The cell proliferation (%) was calculated and compared with control.

Measurement of the half inhibitory concentration and the fold change

The half maximal inhibitory concentrations (IC_{50}) values were obtained by plotting the percentages of A549 and WI-38 cell viabilities versus the concentrations of the sample

using polynomial concentration-response curve fitting models (OriginPro 8 software). The fold changes of IC_{50} values of FEO nanoemulsions relative to the neat unformulated pure FEO (F0) and the positive control (reference drug, DOX) were calculated for all cells.

Flow cytometry-based apoptosis assay

Flow cytometry was used to detect the early and late apoptotic cell distributions and healthy populations. Lung cancer A549 and normal WI-38 cells were seeded at a density of 1×10^6 cells and incubated for 24 h. Cells were treated with the IC_{50} of the F0, F1, F2, PIN, and DOX and cultivated for 24 h incubation. After 1 day, all cells were stained with Annexin V FITC and propidium iodide (PI) (Thermo Scientific). The apoptosis of the treated and untreated cells was analyzed by flow cytometer (Beckman Coulter Instrument, USA). 25,000 events were recorded per each sample. Apoptotic distributions were measured using Flow Cytometry and analyzed using FlowJo-V10 software.

Quantitative Reverse transcription-polymerase chain reaction (qRT-PCR)

Total RNA Extraction: Total RNA was extracted from A549 and WI-38 cells at a density of 1×10^6 cells using the Invitrogen RNA Purification kit (Thermo Fisher) according to the manufacturer's protocol. Cells were applied with the IC_{50} dosage of the proposed treatments and incubated for 24 h. The concentration and the purity of RNA were assessed by Nanodrop Technologies at 260/280 ratio.

Conversion of RNA to cDNA: First-strand cDNA was synthesized with 1 μ g of total RNA using a RevertAid First strand cDNA synthesis kit (Thermo Fisher Scientific, USA) in accordance with the manufacturer's instructions.

Real-Time PCR reactions: Quantitative real-time PCR was performed using the MiScript SYBR Green PCR kit which was purchased from (Qiagen, USA), in addition to the forward and reverse primers for each gene. The nucleic acid sequences of the forward (F) and reverse (R) primers of DR5, FAAD, Caspase 8 (Cas8), p53, Bax, Bcl-2, NF- κ B, and STAT-3 genes compared to GAPDH as a housekeeping gene are illustrated in Table 1.

Real-time PCR mixture consisted of 10 μ l of SYBR PCR Master Mix, 1 μ l of F primer, 1 μ l of R primer, 1 μ l cDNA, and 7 μ l Rnase-free water in a total volume of 20 μ l. Amplification conditions and cycle counts were a temperature of 95 $^{\circ}$ C for 15 min for the initial qPCR step, followed by 35 cycles of denaturation at 95 $^{\circ}$ C for 30 s, annealing at 55 $^{\circ}$ C for 30 s, and elongation at 72 $^{\circ}$ C for 30 s. Melting curves were performed after qPCR to demonstrate the specific amplification of the genes of interest. Relative fold changes in the expression of the proposed genes were accomplished using the comparative $2^{-\Delta\Delta Ct}$ with the housekeeping GAPDH gene to normalize the expression levels. $\Delta\Delta Ct$ is the difference between the mean ΔCt (treatment group) and mean ΔCt (control group), where ΔCt is the difference between the mean CT gene of interest and the mean CT internal control gene in each sample.

Measurements of ROS markers

Nitric oxide (NO)

After treatments with F0, F1, F2, PIN, and DOX, nitric oxide (NO) of lung cancer A549 and normal lung WI-38 cell lines was measured using NO colorimetric kit

Table 1 Primer sequences for real time qRT-PCR

Gene	Primer sequence	
DR5	F	5'-CCAGCAAATGAAGGTGATCC-3'
	R	5'-GCACCAAGTCTGCAAAGTCA-3'
FADD	F	5'-CTCAGGTCCTGCCAGATGAAC-3'
	R	5'-GGACGCTTCGGAGGTAGATG-3'
Caspase8	F	5'-AGAGTCTGTGCCAAATCAAC-3'
	R	5'-CTGCTTCTCTTTGCTGAA-3'
P53	F	5'-GTCTATAGGCCACCCC-3'
	R	5'-GCTCGACGCTAGGATCTGAC-3'
Bax	F	5'-ATGGCTTCTATGAGGCTGAG-3'
	R	5'-CGGCCCCAGTTGAAGTTG-3'
Bcl-2	F	5'-CTGCACCTGACGCCCTTACC-3'
	R	5'-CACATGACCCACCGAACTCAAAGA-3'
NF- κ B	F	5'-ATGGCTTCTATGAGGCTGAG-3'
	R	5'-GTTGTTGTTGGTCTGGATGC-3'
STAT-3	F	5'-CATATGCGGCCAGCAAAGAA-3'
	R	5'-ATACCTGCTCTGAAGAACT-3'
GAPDH	F	5'-GTCTCCTCTGACTTCAACAGCG-3'
	R	5'-ACCACCTGTTGCTGTAGCCAA-3'

F = forward primer

R = reverse primer

(Bio-Diagnostics Co., Egypt) according to Abd-Rabou et al (2020). Nitric oxide (NO) is rapidly oxidized into nitrite and nitrate which are used to quantitate NO production. In details, both cell lines were cultured in 96-well plates at a density of 1×10^4 cells/well. In the second day, the IC_{50} dosages of the proposed treatments were added in the media. Nitrate reductase was first used to convert nitrate to nitrite. Then, Griess reagent was used to convert nitrite to a deep purple azo compound. The amount of the azo chromophore accurately reflected NO amount in the samples. Finally, optical density was measured at 540 nm using the microplate reader (BMG Labtech, Germany).

Inducible nitric oxide synthase (iNOS)

iNOS enzyme activity of A549 and WI-38 cells were measured after treatments with F0, F1, F2, PIN, and DOX using ELISA kit (Wuhan Fine Biotech Co., China). The provided microtiter plate has been pre-coated with target. During the reaction, target in the sample or standard competes with a fixed amount of target on the solid phase supporter for sites on the Biotinylated Detection Antibody specific to target. Excess conjugate and unbound sample or standard were washed from the plate, and HRP-Streptavidin (SABC) was added to each microplate well and incubated. Then substrate solution is added to each well. The enzyme-substrate reaction is terminated and the color change is measured spectrophotometrically at absorbance A_{450} nm. The concentration of iNOS in the samples is then determined by comparing the absorbance of the samples to the standard curve.

Statistical analysis

Results of FEO isolation, analysis and formulation of nanoemulsions were an average of at least two replications \pm standard deviation (SD). On the other hand, Results of the biological activity (represented as graphs) were conducted using the one-way ANOVA (SPSS program, version 21). Bars in all graphs were represented as mean of three different experiments ($n = 3$) \pm SD. Significant difference between treated groups and control means p value less than 0.05.

Results and discussion

Characterization of frankincense essential oil (FEO)

Distillation of frankincense oleogum gave a colorless transparent essential oil having a characteristic spicy-woody aroma similar to its parent oleogum. The yield of FEO was $5\% \pm 0.05$ (w/w), which came in accordance with the literature which indicates that the oil yield can vary between 5 and 15% (Mertens et al. 2009). Table 2 shows that α -pinene is the major constituents of FEO ($\sim 60\%$) as determined by GC-FID and identified by GC-MS analysis. This result came in agreement with Woolley et al. (2012) who previously confirmed that this compound is the major volatile compound of FEO (68%), and is linked specifically to frankincense which belongs to *Boswellia sacra* species. On the other hand, Van Vuuren et al. (2010) reported lower content of α -pinene from *B. sacra* ranging between 18 and 22% and even much lower value (5.3%) was also reported for FEO from the same species (Al-Harrasi and Al-Saidi 2008). In fact, the amount of α -pinene varies radically not only among the 17 species of genus *Boswellia* (Mertens et al. 2009) but also varies within the same *B. sacra* species (Van Vuuren et al. 2010). That is due to the variation of the geographical location, climate, harvest conditions in addition to other factors (Mikhaeil et al. 2003). Therefore, it is important to correlate the results of the anti-lung cancer activity of FEO which will be reported in the current investigation to the chemical composition illustrated in Table 2, rather than to generalize it to any other *B. sacra* species.

Table 2 Chemical composition of FEO as revealed by GC-FID and GC-MS analysis

Identified compounds*	Area % (after FID)
α -Pinene	59.5 ± 0.9
Camphene	1.99 ± 0.01
Sabinene	4.4 ± 0.09
β -Pinene	1.67 ± 0.04
β -Myrcene	0.27 ± 0.001
delta-3-Carene	2.43 ± 0.04
p-Cymene	1.01 ± 0.02
Limonene	4.99 ± 0.1
<i>Cis</i> (or <i>trans</i>) verbenol**	3.89 ± 0.06
Total identified compounds	80.10%

* Using GC-FID and GC-MS by comparing their retention time with standard samples and by matching their mass spectrum with those of standards stored in the electronic mass library

** Identified by GC-MS only with matching percentage 94% with the standard MS of that compound stored in the mass library

Characterization of FEO nanoemulsions

The low energy emulsification technique was used for the fabrication of two formulas of FEO nanoemulsions, namely, F1 and F2. This technique is simple and requires no high shear equipment for fabrication, instead it just requires a fine management of some parameters related to the interfacial properties of the system. That include surfactant type, the ratio between surfactant and the essential oil, incorporation of Ostwald ripening inhibitor and co-surfactant (Edris 2021). Visual inspection of the nanoemulsions (F1 and F2) right after formulation indicate that both nanoemulsions exhibited a bluish fluorescence with translucent appearance (Fig. 1b). That manifest a Tyndall scattering effect which is a visual characteristic which indicates the formation of nanoparticles. During storage at room temperature, both nanoemulsions tend to equilibrate gradually until exhibiting a crystal-clear transparent appearance (Fig. 1c), which confirms the occurrence of major population of FEO nanoparticles having diameter < 100 nm. No sign of phase separation, cloudiness nor opaqueness were detected during storage for 6 months at room temperature indicating high kinetic stability toward gravitational separation.

Figure 1d illustrates the particle size distribution of FEO nanoemulsions at the zero time and after 6 months of storage. At the zero time (left), both nanoemulsions showed bimodal size distribution in which particles are distributed among two populations. The first is a major intense population (85%–90%) with particles ~ 10.0–20.0 nm, and the second has less intense population (9–12%) with particles > 100 nm. Nanoemulsion F1 which was fabricated without the co-surfactant (PG) had z-average (d. nm) 95.57 ± 0.3 with poly-dispersibility index 0.162. On the other hand, nanoemulsion F2 that contained 1% (PG) had a z-average (d.nm) 28.7 ± 1.9 , and poly-dispersibility index 0.32.

TEM photos (Fig. 1e) confirm the major nano-size population (< 100 nm) of F1 and F2.

After 6 months of storage (Fig. 1d, right), a large population of nanoparticles (10–20 nm) was still prevailing indicating no aggregation and high stability. It was interesting to find that the size distribution of nanoemulsion F2 improved after storage, so that it eclipsed with the size distribution of F1 to become almost the same pattern. This indicates that during storage particles are equilibrating continuously till reaching their final size distribution pattern. That behavior was confirmed visually in Fig. 1b, c and also in our previous investigation (Abd-Rabou and Edris 2021).

Assessment of the cytotoxicity

The cytotoxic effect of pure unformulated FEO (F0) and its two formulated nanoemulsions (F1 and F2) as well as α -pinene (PIN), the main volatile constituent of FEO, and doxorubicin (DOX), a positive control, was evaluated against lung cancer A549 cells and normal lung WI-38 cells. The former cell lines are commonly used as a model for in vitro evaluation of cytotoxicity of the non-volatile fraction of frankincense (boswellic acids), which is a potential candidate for lung cancer treatment (Minghe et al. 2020). The cytotoxicity effect in the current investigation was evaluated and represented in two terms, namely, cell proliferation percentage (Fig. 2a–d) and IC_{50} values (Table 3). The results of these two evaluations accompanied by discussion and rationalization are presented in the next passage.

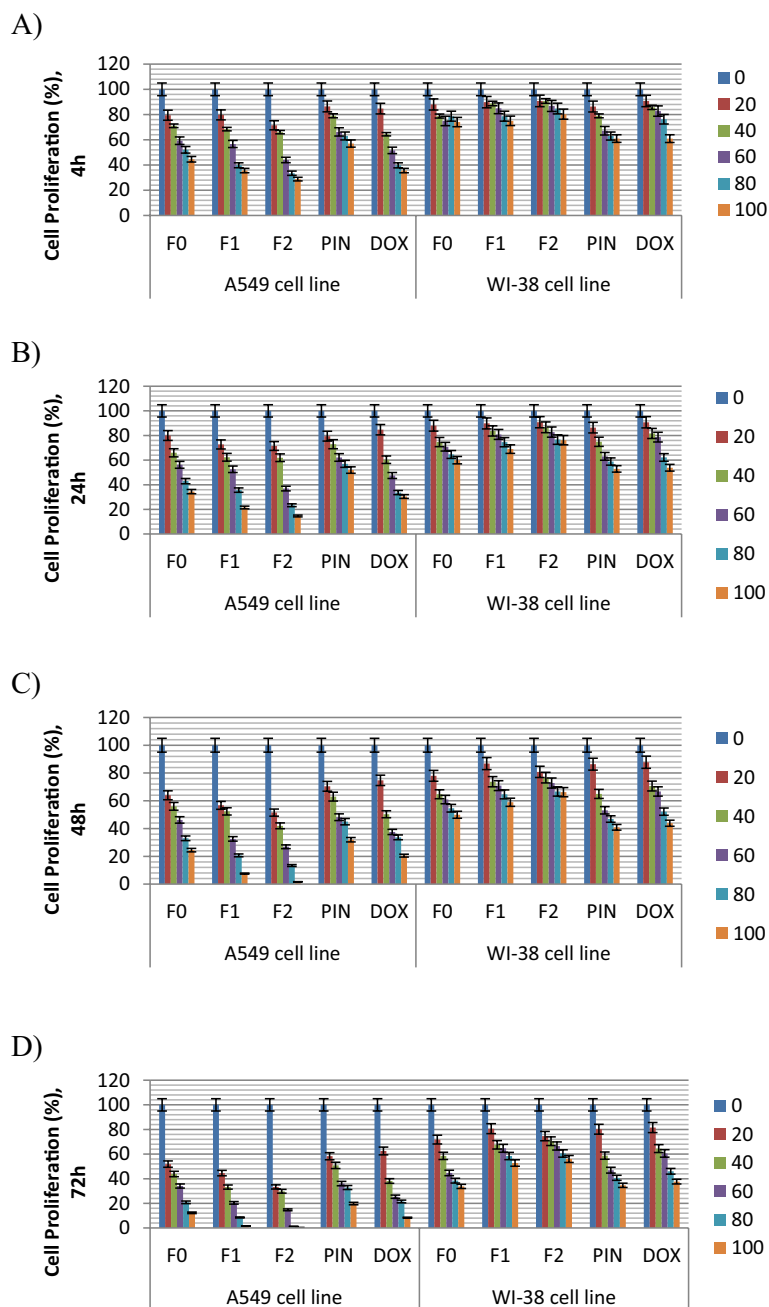


Fig. 2 Cytotoxicity of different doses (0–100 µg/ml) of the tested formulas against lung cancer cell lines (A549) versus normal WI-38 cells. Cells were incubated with these formulas for 4 h (A), 24 h (B), 48 h (C), and 72 h (D)

Cytotoxicity of pure unformulated FEO (F0)

The results in Fig. 2 generally revealed that there is a significant ($P < 0.05$) dose-dependent and time-dependent decrease in cancer A549 cell proliferation percentage upon treatment with F0 after 4 h (Fig. 2a), 24 h (Fig. 2b), 48 h (Fig. 2c), and 72 h (Fig. 2d) incubation periods. FEO (F0), after 4 h incubation with 100 µg FEO/ml, inhibited cell proliferation to 44.54% and 74.02% for cancer A549 and normal WI-38 lung cells, respectively

Table 3 IC₅₀ and fold changes of lung cancer A549 and normal WI-38 cell lines upon different treatments

Incubation period	IC ₅₀ and fold changes	Lung cancer cell line					Normal cell line				
		F0	F1	F2	PIN	DOX	F0	F1	F2	PIN	DOX
4 h	IC ₅₀	64.11	60.34	52.15	72.47	58.03	77.81	85.62	88.10	72.39	84.64
	FC1	1.0	1.06	1.23	0.88	1.10	1.0	0.91	0.88	1.07	0.92
	FC2	0.91	0.96	1.11	0.80	1.0	1.09	0.99	0.96	1.17	1.0
24 h	IC ₅₀	60.12	55.42	47.07	66.27	54.11	72.98	81.85	83.65	69.19	79.16
	FC1	1.0	1.08	1.28	0.91	1.11	1.0	0.95	0.93	1.12	0.98
	FC2	0.90	0.98	1.15	0.82	1.0	1.08	0.97	0.95	1.14	1.0
48 h	IC ₅₀	47.89	38.72	30.50	54.58	45.38	62.07	72.47	72.74	60.21	68.65
	FC1	1.0	1.24	1.57	0.88	1.06	1.0	0.86	0.85	1.03	0.90
	FC2	0.95	1.17	1.49	0.83	1.0	1.11	0.95	0.94	1.14	1.0
72 h	IC ₅₀	34.60	22.22	14.88	41.29	32.09	50.30	65.70	66.34	53.44	61.88
	FC1	1.0	1.56	2.32	0.84	1.08	1.0	0.77	0.76	0.94	0.81
	FC2	0.93	1.44	2.16	0.78	1.0	1.23	0.94	0.93	1.16	1.0

FC1: Fold change (1), the ration between IC₅₀ of F0 to that of all other tested formulas and compounds

FC2: Fold change (2), ration between the IC₅₀ DOX to that of all other tested formulas and compounds

(Fig. 2a). The highest cytotoxic effect appeared after 72 h incubation period at 100 µg/ml, where cell proliferation reached 12.33% and 33.77% for cancer A549 and normal WI-38 lung cells, respectively (Fig. 2d).

Regarding cytotoxicity of F0 in terms of IC₅₀, results in Table 2 indicates that 34.60 µg/ml of FEO is required to eradicate half population (50%) of lung cancer A549 cells after 72 h incubation period. On the other hand, 50.30 µg/ml is required to do the same effect in case of WI-38 normal cell line. Results in Table 3 also showed that lung cancer cells were more sensitive to FEO compared to the normal lung cells. This observation was also reported for FEO (belong to the same *sacra* species) against some breast cancer cells (Suhail et al. 2011). However, we wanted to compare our results with relevant investigations which also evaluate FEO against lung cancer A549 cells, rather than any other cancer cell type. Unfortunately, these key investigations are seldom, which makes our study an initiative (first report) that exhibits the potentials of FEO (from *B. sacra*) as a cytotoxic plant-based volatile oil against lung cancer non-small cells (A549).

In general, the biological activity of plant extracts is directly linked to their chemical composition and their active principles. Regarding FEO, the major volatile constituent was found in this investigation to be α-pinene (PIN) which represent ~60% of the total essential oil composition (Table 2). This volatile monoterpene compound showed cytotoxic activity against different types of cancer cells (Kumar et al. 2021; Zhao et al. 2018; Chen et al. 2015). It exerts its activity through induction of cell cycle arrest and apoptosis. Concerning previous investigation on lung cancer cells, it was reported that α-pinene (individually) did not produce significant cytotoxicity on lung cancer A549 cells (Zhang et al. 2015). However, combining α-pinene with a protocol-prescribed anti-lung cancer drug like paclitaxel enhanced the cytotoxicity of the drug against these cancer cells by synergistic effect (same reference).

Based on that notification, the authors of the current study included individual α-pinene (PIN) in the cytotoxicity evaluation along with FEO (Fig. 2a–d and Table 2),

to compare their activity. Results showed that FEO (F0) inhibited cancer cell proliferation percentage compared to PIN after 4 h up to 72 h, indicating higher cytotoxic effect. This result is also confirmed through the IC_{50} evaluations (Table 3) which showed that after only 4 h incubation period the IC_{50} was 64.1 for F0 versus 72.4 for PIN with a fold change 0.88.

After 72 h, the IC_{50} value was further decreased to 34.6 and 41.2 for F0 and PIN, respectively, with a fold change 0.84. These results indicate that FEO which contains only ~60% α -pinene is more cytotoxic to A549 lung cancer cells than pure individual α -pinene. That is most probably due to the synergistic effect between α -pinene inherently present in FEO and the other neighboring volatile components which all together constituents that oil. Here, we would like to point out to the fact that 80.1% of FEO volatile compounds were identified (Table 2), while 19.9% minor compounds are still unknown, which may also participate in the anti-lung cancer activity of FEO.

Even though the fold change of IC_{50s} between FEO and PIN is only 0.8, formulation of the former in nanoemulsion form will increase this value and make FEO is unexchangeable with pure individual α -pinene, as will be manifested in the next passage.

Cytotoxicity of FEO nanoemulsion (F1)

Water-based nanoemulsions afford administration and delivery of lipophilic drugs through aqueous media (like blood) via intravenous injection. In addition, drug nanoparticles can enhance the cytotoxic activity of drugs due to better diffusion of nanoparticles into the cancer cells, as was proven in our previous investigation (Abd-Rabou and Edris 2021). Therefore, FEO in the current study was formulated in two water-based nanoemulsions, namely, F1 and F2, which differ from one another in the content of the co-surfactant, propylene glycol (PG), as described previously.

Regarding F1 (formulated without PG), it was found that this nanoemulsion inhibited cell proliferation of lung cancer cells to become 35.59% after 4 h incubation at 100 μ g FEO/ml (Fig. 2a). This inhibition in cancer cell proliferation was almost equals to that caused by the reference drug DOX (35.60%), but lower than that caused by α -pinene (PIN, 57.2%). On the other hand, normal lung cells were less affected by F1, where cell proliferation was kept at 75.02%, under the same conditions. Both cells proliferation was inhibited gradually in time-dependent manner until reaching the highest inhibition after 72 h incubation. At that time, the proliferation of lung cancer cells was greatly inhibited by F1 to reach only 1.61%, at the highest tested dose. That indicates more cytotoxic effect compared to BIN and the reference drug DOX, which both showed cell proliferation at 19.8% and 8.3%, respectively. Meanwhile, the proliferation of normal lung cells was less affected (52.77%) by nanoemulsion F1 after 72 h incubation period (Fig. 1d).

In line with these results, Table 3 also confirmed the previous finding, where the IC_{50} of F1, BIN and DOX after 72 h incubation was 22.22, 41.2 and 32.09 μ g FEO/ml, respectively. On the other hand, the IC_{50} of F1 for normal lung cells was 65.70 μ g FEO/ml under the same conditions.

Comparing the cytotoxicity of pure unformulated FEO (F0) with that of FEO nanoemulsion (F1) one can clearly observe the enhanced cytotoxic effect of the latter due to its content of nanoparticles. Cell proliferation of lung cancer cells were almost ceased after

72 h incubation (Fig. 2d) with nanoemulsion F1. That indicates higher cytotoxicity than F0, where cell proliferation reached 12.3% after the same incubation period.

More interestingly, the cytotoxicity of nanoemulsion F1 surpassed that of the reference drug DOX in which about 8.3% lung cancer cell were still proliferating after 72 h incubation period with the drug.

Regarding cytotoxicity in terms of IC_{50} values, Table 2 indicates that this value was always lower for nanoemulsion F1 compared to F0, PIN and DOX throughout the whole incubation periods.

Cytotoxicity of FEO nanoemulsion (F2)

FEO nanoemulsion F2 has the same composition as F1 with an extra ingredient incorporated within the formula which is 1.0% PG. This compound was used commonly as a co-surfactant to facilitate nanoemulsion formation as was previously indicated (Edris 2021). However, we noticed that it was possible to formulate FEO nanoemulsion even without using PG, as the case of nanoemulsion F1. This observation indicates that FEO has an inherent tendency to lend itself easily to nanoemulsion formation. That could be due to the compatibility between the chosen surfactant (Cremophor RH40) with the ingredients of the essential oil (FEO), in the sense of their hydrophilic-lipophilic balance (Tokuoka et al. 1993).

In the current section we are going to evaluate if there is any difference in cytotoxicity following the incorporation of PG in nanoemulsion F2, compared to the unformulated FEO (F0), PG-free nanoemulsion (F1), α -pinene (PIN), and the drug (DOX).

Figure 2a indicates that F2 inhibited lung cancer cells proliferation to a higher extent compared to F0, F1, PIN and DOX at all incubation periods. After 48 h incubation, nanoemulsion F2 at the highest dose was able to induce profound inhibition toward cancer cell proliferation, while F0, F1, PIN and DOX treated cells were still proliferating at 24.4%, 7.5%, 31.9% and 20.5%, respectively (Fig. 2c). After 72 h incubation period nanoemulsions F1 and F2 were the only tested formula which were able to inhibit (almost completely) the cell proliferation of cancer cells (Fig. 2d).

Results illustrated in Table 3 confirmed the previous data, where the IC_{50} of both F1 and F2 were the lowest (22.22 and 14.88 μ g of FEO/ml, respectively) among the other tested compounds after 72 h incubation period.

From the same table, it can be noticed that F2 recorded the highest fold change (FC1), where there is 2.32-fold increase of F2 compared to F0 and 2.16-fold increase (FC2) compared to the drug DOX. For normal lung WI-38 cells, there is 0.94-fold decrease (FC1) of F2 compared to F0 and 0.93-fold decrease (FC2) of F2 compared to DOX.

It is clear from the above-mentioned results that PG has a significant role in increasing the cytotoxicity of FEO nanoemulsion (F2). The mechanism of action could be similar to that which was previously reported by Zhao et al. (2013) for PG-liposomes delivery system against multidrug resistant cancer cells. They postulated that PG has potentials to improve membrane permeability and to increase the fluidity and flexibility of liposomes to make it more deformable and more easily being taken by cancer cells. Regarding incorporation of PG in the nanoemulsion, it was reported that this compound has the ability to arrange itself along with the main surfactant used for emulsion formation at the interfacial layer between the oil and water phases (Garti et al. 2001). That orientation

(Fig. 3) leads to the formation of a mixed surfactant film which is more flexible than single-surfactant film. This behavior imparts more flexibility and fluidity to FEO nanoparticles in nanoemulsion F2 to diffuse through the cell wall of cancer cells easier than F1, as predicted from the enhanced cytotoxicity of F2.

It is worth to indicate that in the previous investigation, Zhao et al. (2013) formulated PG-liposomes containing 16% PG. On the other hand, in our current investigation, nanoemulsion F2 was fabricated using only 1.0% PG. This gives a preliminary indication that more PG in FEO nanoemulsion may potentially manifest even more cytotoxic effect than that reported in the current study. However, that hypothesis must be verified through a complementary investigation which we plan to conduct in the next project.

Cytotoxicity and safety of FEO and its nanoemulsions on normal lung cells WI-38

The major liability of chemotherapeutic drugs is the lack of selectivity which leads to deleterious effects on normal tissues. Therefore, finding tumor-specific therapy which can target only cancer cells, while sparing normal cells is a prerequisite. Based on that, in the current study, the cytotoxicity of FEO along with the other tested formulas was also evaluated against the normal WI-38 lung cells to estimate the safety of these formulas.

Figure 2a indicates that after 4 h incubation period, the drug DOX and α -pinene PIN, at the highest dose, were more cytotoxic to normal lung cell, where cell proliferation was inhibited to 60.9% in both cases. On the other hand, F0, F1, and F2 were less cytotoxic to normal lung cells with significantly higher cell proliferation percentage (74.0%, 75.0% and 80.2%), respectively. After 72 h incubation, the cytotoxicity of DOX and PIN was further increased, and consequently normal cell proliferation decreased to reach 37.6% and 34.7%, respectively. Meanwhile, F0, F1 and F2 showed relatively less cytotoxic effect with higher cell proliferation percentage reaching 33.7%, 52.7% and 56.0%, respectively. Table 3 illustrates a larger safety limit of F1 and F2 toward normal lung cells, where the IC_{50} values (65.70 and 66.34 μ g of FEO/ml) were the highest among the other tested compounds after 72 h incubation period.

Therefore, it is obvious that FEO nanoemulsion F2 was relatively the least cytotoxic among all tested compounds against normal lung cells. Interestingly the very same nanoemulsion was also manifested the highest cytotoxicity against lung cancer cell as shown previously, indicating the specific attitude of nanoemulsion F2. Data in Table 3 regarding cytotoxicity in terms of IC_{50} values confirmed the same results.

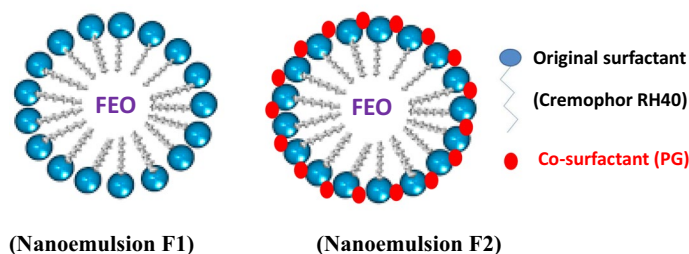


Fig. 3 Schematic representation of single surfactant film (F1) and PG-mixed surfactant film (F2) of FEO nanoemulsions

It is well known that p53 activation protects normal cells from the cytotoxicity of chemotherapy through modulation of cell cycle checkpoints (S-phase or M-phase). This idea opened a therapeutic window in developing new anti-cancer candidates (e.g., nanoemulsion F2 in the current study), which can up-regulate p53 gene expression. That is in one direction induce apoptosis in cancer cells, while in another direction, keep normal cells healthy through regulation of their cell cycle checkpoints (Cheok 2012).

Apoptosis

After studying the cytotoxic effect of FEO and its two nanoemulsions against lung cancer A549 and normal lung WI-38 cells, this section investigates the mechanistic approach of killing lung cancerous cells. That approach was fulfilled through flow cytometric analysis together with genetic expressions of pro-apoptotic (DR5, FAAD, Caspase 8 (Cas8), p53, and Bax) and anti-apoptotic (Bcl-2, NF- κ B, and STAT-3) gene markers.

Flow cytometric analysis

Flow cytometric analysis is a laser-based technique used to detect and measure physical and chemical characteristics of a population of cells. It is one of the most popular applications of studying programmed cell death (apoptosis). The apoptotic diagrams of lung cancer A549 and normal lung WI-38 cells (Fig. 4a, b) along with their graphical representation (Fig. 4c–f) after treatment with the different FEO formulations, were presented.

From Fig. 4a, b, it is evident that the count percent of lung cancer A549 cells in the quadrant of negative annexin V/negative PI were decreased gradually after treatment with F0, F1, and F2, respectively. Figure 4c shows the un-apoptotic lung cancer A549 cells upon different treatments, recording gradual decrease in a significant manner after treatment with F0, F1, and F2, respectively, with highest reduction observed for nanoemulsion F2 (47.4%). Thus, there was more than half percentage of lung cancer A549 cells that shifted toward apoptosis. On the other hand, pure α -pinene (PIN) and the drug (DOX) recorded an inhibition in the un-apoptotic A549 cells approximately similar to the effect of F0, (around 70%).

For normal lung WI-38 cells, F2 (89.3%) and F1 (85.0%) recorded a non-significant decrease in the un-apoptotic population. Thus, there was very low percentage (around 10.0%) of normal cells that shifted toward apoptosis.

Figure 4d shows the cells that stained with Annexin V dye, i.e., early apoptotic cells, indicating that FEO nanoemulsions F2 followed by F1 induced the highest early apoptosis on lung cancer A549 cells, with the highest percentage shown for F2 (51.6%). Figure 4e shows the cells that stained with propidium iodide dye, i.e., necrotic cells, indicating that F1 followed by DOX then F0 induced little necrosis in A549 cells, with the highest percentage found for nanoemulsion F1 (0.13%). Figure 4f shows the cells that stained with both Annexin V and propidium iodide dyes, i.e., late apoptotic cells. The

(See figure on next page.)

Fig. 4 Apoptotic screening using flow cytometry of the tested formulas against lung cancer A549 versus normal WI-38 cells. **A** apoptotic diagrams of A549 cells, **B** apoptotic diagrams of WI-38 cells. **C** Cells did not stain with dyes and named un-apoptotic cells, **D** cells stained with Annexin V and shifted to early apoptosis, **E** cells stained with propidium iodide (PI) and shifted to necrosis, **F** cells stained with Annexin V and PI and shifted to late apoptosis ($n = 3$)

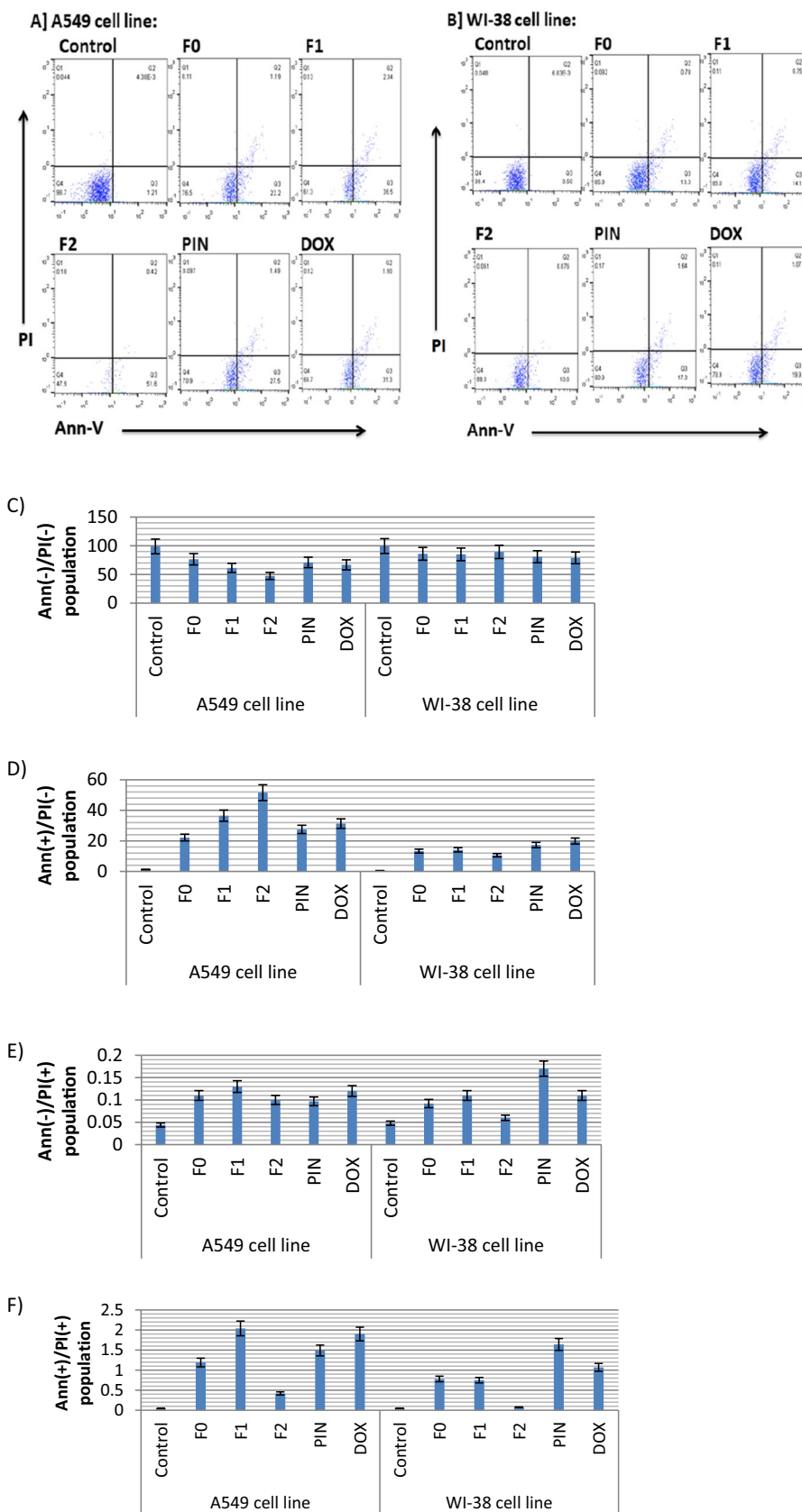


Fig. 4 (See legend on previous page.)

figure indicates that F2, F1, PIN and DOX, induced apoptosis in A549 cells, with the highest percentage in F1 (2.04%).

Some essential oils can promote depolarization of the mitochondrial membranes lead to abnormal permeability of the membranes resulting in leakage of pro-apoptotic factors, such as radicals, cytochrome c, calcium ions and proteins, causing induction of apoptosis (Yaman et al. 2021). It was reported that some terpenes from aromatic plants (e.g., α -pinene) can induce a rapid loss in the membrane potential and activate caspases 3,6, and 7, leading finally to induction of apoptosis (Bock and Tait 2020). Parallel to this finding, Zhang et al. (2015) indicated that the combination therapy with α -pinene and β -pinene showed a synergistic effect on apoptosis against lung A549 cells.

Genetic expression

Gene expression of DR5, FAAD, Cas8, and p53

Genetic expressions of pro-apoptotic (DR5, FAAD, Caspase 8 (Cas8), p53, and Bax) and anti-apoptotic (Bcl-2, NF-kB, and STAT-3) gene markers were evaluated in the current study (Figs. 5, 6, 7) to support the results obtained from the previously discussed apoptotic diagrams (Fig. 4). These genes are called extrinsic apoptotic genes which are different from the intrinsic Bax and Bcl-2 genes, which were also studied in the current investigation, (next section).

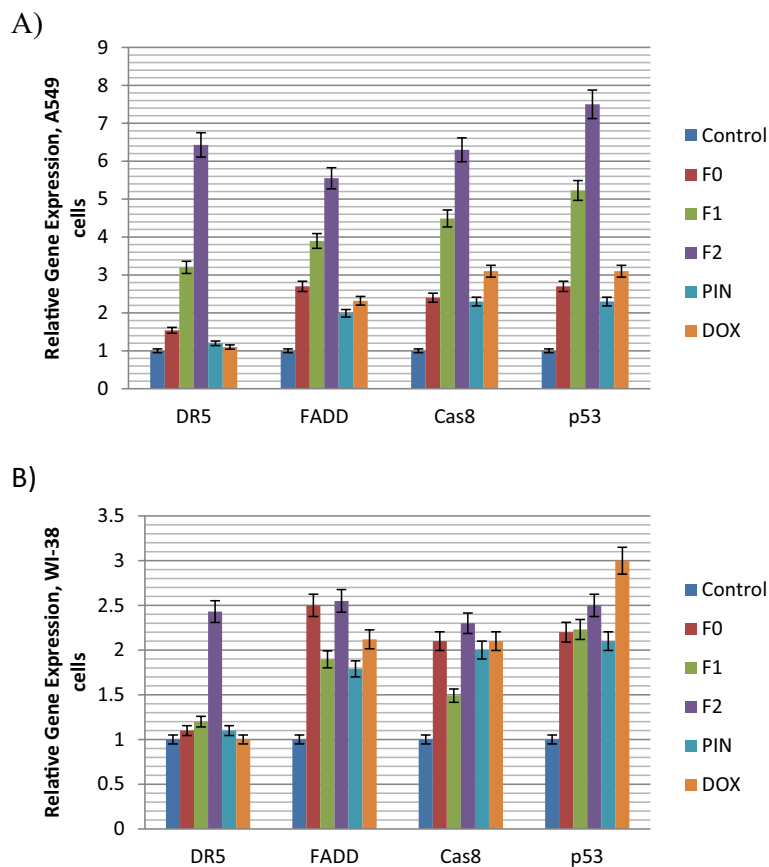


Fig. 5 Genetic expression of pro-apoptotic pathway, **a** in lung cancerous A549 cells, and **b** in normal lung WI-38 cells

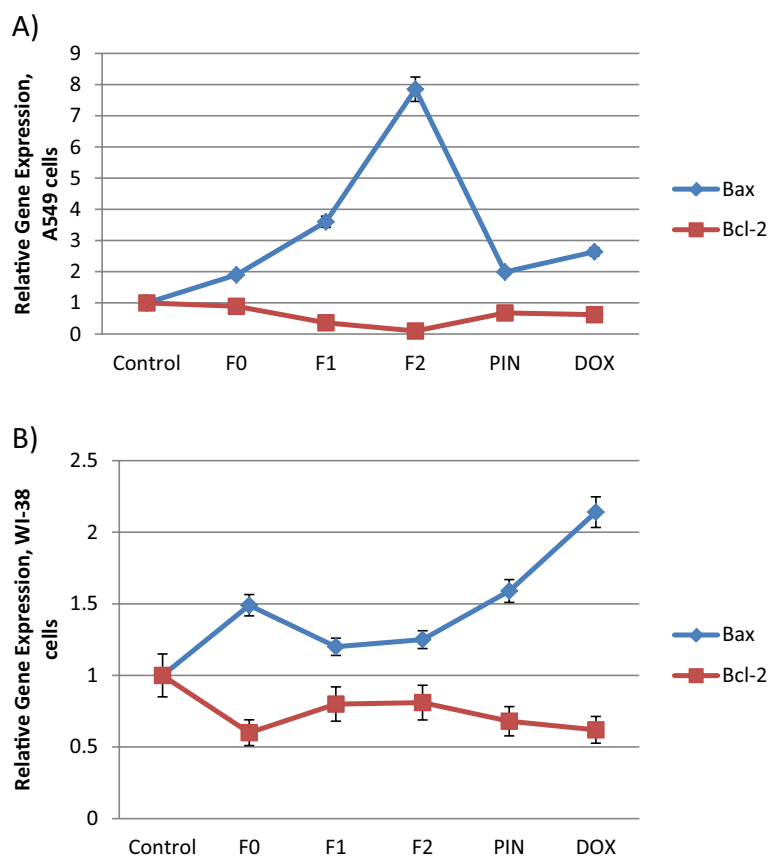


Fig. 6 Genetic expression of pro-apoptotic Bax and anti-apoptotic Bcl-2 genes. **A** In lung cancerous A549 cells and **B** in normal lung WI-38 cells (n = 3)

Tracking the apoptotic pathway in lung cancer A549 cells (Fig. 5a) reveals that F0, F1, F2, and PIN upregulate DR5 expression, which is a proapoptotic death receptor. The relative gene expression was significantly increased only in case of F2 (6.43) compared to control (1). Regarding normal lung WI-38 cells, F2 also induced the DR5 gene expression to a lesser extent (2.43) compared to lung cancer A549 cells (Fig. 5b). This result indicates that F2 perform its killing action against lung cancer cells through DR5-mediated apoptotic pathway. This data came in accordance with a previous study (Lu et al. 2008) which indicate that boswellic acid from non-volatile fraction of frankincense can inhibit tumor cell growth and to induce apoptosis in prostate cancer cells through activation of DR5-mediated apoptotic pathway.

Activation of DR5 using FEO nanoemulsions (F1 and F2) in case of lung cancer A549 cells can produce apoptotic signals through their intracellular death domain (DD) (Gasparian et al. 2009). That is followed by receptor clustering leading to the recruitment of Fas-associated protein with death domain (FADD) (Abbas and Larisch 2020). In the current study, FADD was upregulated using all the tested formulations in lung cancer A549 cells, with the highest gene expression was for nanoemulsion F2 (5.55) compared to control (1), (Fig. 5a).

FADD adaptor protein recruit pro-caspase-8 forming the death-inducing signaling complex (DISC) known as the primary complex. The recruitment of pro-caspase-8

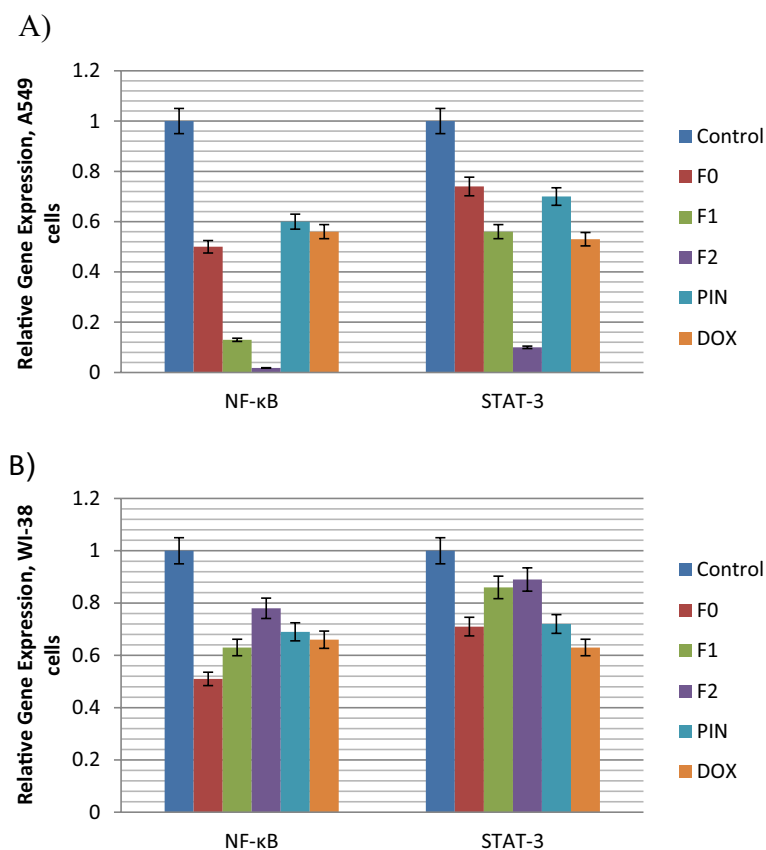


Fig. 7 Genetic expression of survival (anti-apoptotic) genes. **a** In lung cancer A549 cells and **b** in normal lung WI-38 cells ($n = 3$)

causes its activation and subsequent cleavage of caspase-3, -6, and -7 leads to membrane blebbing, DNA fragmentation and nuclear shrinkage (Abbas and Larisch 2020). Thus, in the current study, caspase-8 was upregulated using all the tested formulations in lung cancer A549 cells, with the highest percentage found in F2 (6.3) compared to control (1) (Fig. 5a). This data was also supported by the same previous study (Lu et al. 2008), which indicate that boswellic acid from frankincense induce apoptosis through activation of caspase-8 which was correlated with increased levels of death receptor (DR5) but not of Fas or DR4.

P53 is considered as one of the major tumor suppressors. The main function of p53 is cancer prevention through controlling cell death pathways (Refaat et al. 2014). The activation of p53 is essential in both cancer cells for their death and normal cells for their survival (Cheek 2012). In the current study, p53 was upregulated after treatment with all the tested formulations in lung cancer A549 cells, with the highest percentage found for nanoemulsion F2 (7.5%) compared to control (1) (Fig. 5a).

Figure 5b shows some upregulation of pro-apoptotic genes in normal lung cells but in much lower extent than the highly significant upregulation that was observed in the cancerous lung cells.

Gene expression of Bax and Bcl-2 genes

Regarding the intrinsic pathway of apoptosis, activated caspase-8 requires the engagement of mitochondrial response in terms of Bax and Bcl-2 genes. In this pathway, active caspase-8 upregulates Bcl-2-associated X protein (Bax), then translocate to the mitochondria. This leads to a change in the mitochondrial membrane polarization and release of cytochrome c (Flores-Romero et al 2022) to form a structure known as apoptosome. This apoptosome is essential for the activation of other caspases (9, 3, 6, and 7) (Refaat et al. 2014). In the current study, we find that Bax levels were upregulated, while Bcl-2 genetic levels were down-regulated after treatment with all tested formulations in lung cancer A549 cells compared to control (Fig. 6).

The ratio of genetic expressions of pro-apoptotic (Bax) and anti-apoptotic (Bcl-2) is very important to confirm the apoptotic effect of any new treatment (Fig. 6). Therefore, this ratio was calculated in the current study and shown in Table 4. The data of lung cancer A549 cells (Fig. 6a) indicates that FEO nanoemulsion F2 has the highest Bax genetic level (7.8) and the lowest Bcl-2 genetic level (0.1) compared to normal lung cells (Fig. 6b). FEO nanoemulsion F1 also has high Bax genetic level (3.6) and the lowest Bcl-2 genetic level (0.35). On the other hand, F1 and F2 had non-significant changes of Bax and Bcl-2 genetic levels (around 1) on WI-38 normal cells.

Bax/Bcl-2 ratio above (> 1) is an indication of apoptotic induction, while ratio below (< 1) is an indication of apoptotic suppression, as shown in Table 4. The table illustrates that nanoemulsion F1 showed lower ratios than F2, compared with normal cells. Nanoemulsion F2 showed the highest Bax/Bcl-2 ratio, recording 78.50 for lung cancer A549 cells and 1.54 for normal WI-38 cells, respectively. On the other hand, F1 came next to F2 in activity, recording Bax/Bcl-2 ratio with 10.00 and 1.5 for lung cancer and normal cells, respectively.

F0, PIN, and DOX also elevate the Bax/Bcl-2 ratio but in a very lower manner compared to both FEO nanoemulsion (F1 and F2). There are no remarkable changes in the Bax/Bcl-2 ratio of F0, PIN, and DOX when comparing lung cancer and normal lung cells (Table 4).

In general, essential oils were able to change expression levels of Bcl-2 and *Bax* genes leading to release of cytochrome C and induction of apoptosis in cancerous cells (Cha et al. 2009). That happens via activation of caspases 9 and 3 which in turn causes apoptosis. Antiapoptotic Bcl-2 protein is downregulated by the action of essential oil on the cancer cells.

Gene expression of NF-kB and STAT-3 genes

Development of chemo-resistance is a well-known phenomenon that may arise after cancer treatment. It leads to reoccurrence of cancer due to the induction of some

Table 4 The ratio of pro-apoptotic (Bax) to the anti-apoptotic (Bcl-2) gene markers (Bax / Bcl-2)

Cell lines	Control	F0	F1	F2	PIN	DOX
Lung cancer A549 cell line	1.0	2.13	10.00	78.50	2.92	4.25
Normal lung WI-38 cell line	1.0	2.48	1.50	1.54	2.33	3.45

survival (anti-apoptotic) genes, such as NF- κ B and STAT-3. Therefore, inhibition of these genes is an attractive therapeutic strategy, which is included in the current study.

Figure 7a indicates that NF- κ B and STAT3 genes were downregulated in lung cancer A549 cells upon treatment with all formulations, recording the highest downregulation with FEO nanoemulsion F2 (0.018 and 0.1, respectively) compared to control (1.0). On the other hand, Fig. 7b shows some non-significant downregulation of survival genes in normal lung cells but in much lower extent compared to that in the case of cancerous lung cells.

Evaluation of reactive oxygen species

Reactive oxygen species (ROS) such as nitric oxide (NO) can cause DNA damage and p53 activation. That leads to direct DR5 upregulation (extrinsic apoptotic pathway) (Kannappan et al. 2010), or activation of Bax upregulation (intrinsic apoptotic pathway) (Park et al. 2013). In addition, DR5 activators can act by the downregulation of NF- κ B and STAT pathways (Nazim et al 2020).

Therefore, measurements of ROS markers such as nitric oxide (NO) and its enzyme, inducible nitric oxide synthase (iNOS) were conducted to study the potentials of both FEO nanoemulsions to induce ROS-mediated apoptosis. Figure 8 shows the levels of NO and iNOS produced by lung cancer and normal cells after treatments with the different formula versus control. Both ROS markers (NO and iNOS) were significantly increased ($P < 0.05$) upon the treatments, with very high significance for nanoemulsion F2 (46.54 and 27.64, respectively) compared to the untreated control (15.6 and 6.7, respectively). On the other hand, nanoemulsion F1 induced also significant elevation of both markers but to a lesser extent (31.37 and 18.39, respectively) compared to the untreated control (15.6 and 6.7, respectively).

Both FEO nanoemulsions showed non-significant increase of NO and iNOS levels in normal lung WI-38 cells (Fig. 8b). This result indicate that the naniemulsions activated iNOS enzyme which induced NO-mediated apoptosis in lung cancer A549 cells but not in normal lung WI-38 cells.

In general, essential oils were reported to induce cancer cell death by increasing ROS production. This phenomenon led to cell death-mediated apoptosis (Sœur et al. 2011). In addition, some terpenes (e.g., α -pinene) inhibited cell proliferation, induce oxidative stress, increased ROS formation, and caused apoptosis (Wang et al. 2021).

Conclusions

Frankincense essential oil rich in α -pinene isolated from *Boswellia sacra* oleogum showed a potential for driving lung cancer A549 cells to apoptosis and prevent reoccurrence. Formulation of that oil in a water-based nanoemulsion in the presence of propylene glycol as co-surfactant enhanced greatly its cytotoxicity against lung cancer cells with minimum effect on normal cells. The results obtained in the current study could be useful in developing a plant-based phytochemical from the volatile fraction of frankincense that can potentially be used as adjuvant in lung cancer chemotherapy.

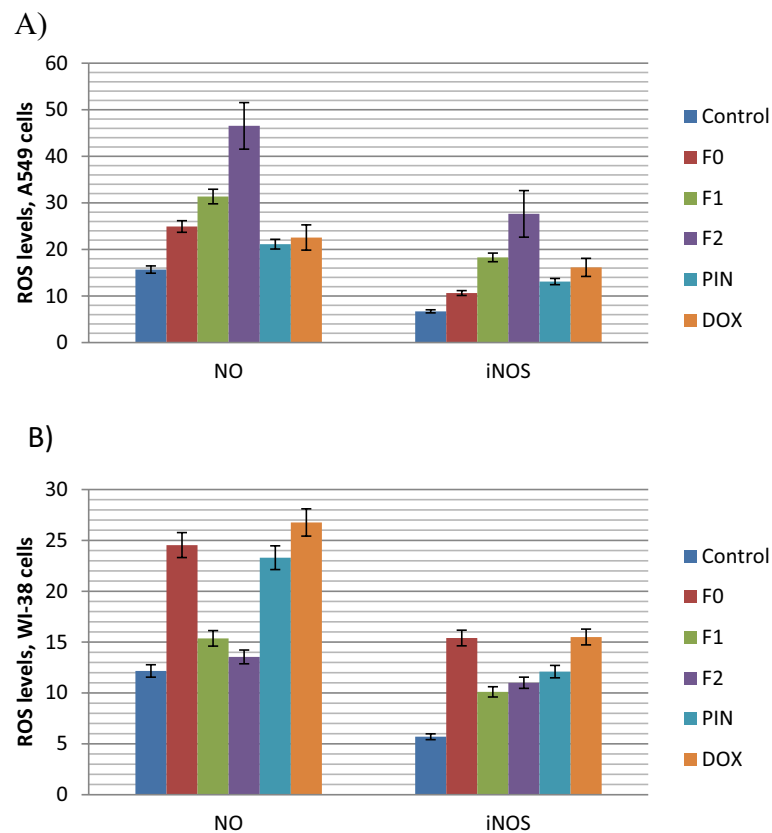


Fig. 8 Reactive oxygen species (ROS) measurements. **A** NO and iNOS enzyme activity levels in lung cancer A549 cells and **B** in normal lung WI-38 cells ($n = 3$)

Acknowledgements

Nothing to acknowledge.

Author contributions

AAA-R and AEE participated equally in the design, data curation, writing and revising of the manuscript. AEE was responsible for extraction, characterization of the plant extract and the formulation and characterization of nanoemulsions. AAA-R was responsible for the evaluation of cell culture, cancer cell propagation and subculturing, anticancer activity, apoptotic experiments, and genetic expressions. Both authors read and approved the final manuscript.

Funding

Open access funding provided by The Science, Technology & Innovation Funding Authority (STDF) in cooperation with The Egyptian Knowledge Bank (EKB).

Availability of data and materials

The data sets used and/or analyzed during this study are available from the corresponding author on reasonable request.

Declarations

Ethics approval and consent to participate

An ethical approval is granted to deal with cell lines from the authority of Medical Institute at the National Research Center, Cairo, Egypt.

Consent for publication

Not applicable.

Competing interests

We declare that the authors have no competing interests as defined by BMC, or other interests that might be perceived to influence the results and/or discussion reported in this paper.

Received: 18 April 2022 Accepted: 22 June 2022

Published online: 11 July 2022

References

- Abbas R, Larisch S (2020) Targeting XIAP for promoting cancer cell death—the story of ARTS and SMAC. *Cells* 9(3):663–677
- Abd-Rabou A, Edris A (2021) Cytotoxic, apoptotic, and genetic evaluations of *Nigella sativa* essential oil nanoemulsion against human hepatocellular carcinoma cell lines. *Cancer Nanotech* 12:28–50
- Abd-Rabou A, Ahmed H, Shalby A (2020) Selenium overcomes doxorubicin resistance in their nano-platforms against breast and colon cancers. *Biol Trace Elem Res* 93(2):377–389
- Al-Harrasi A, Al-Saidi S (2008) Phytochemical analysis of the essential oil from botanically certified oleogum resin of *Boswellia sacra* (Omani Luban). *Molecule* 13:2181–2189
- Bittoni M, Bibi A, Williams N, Mendelson M, Grainger E et al (2021) P4003 Report on a phytochemical-rich dietary intervention trial to prevent lung cancer: Implementation in a high-risk lung screening clinic. *J Thorac Oncol* 16(3):S470–S471
- Bock F, Tait S (2020) Mitochondria as multifaceted regulators of cell death. *Nat Rev Mol Cell Biol* 21(2):85–100
- Börner F, Werner M, Ertelt J, Meins J, Abdel-Tawab M et al (2021) Analysis of boswellic acid contents and related pharmacological activities of frankincense-based remedies that modulate inflammation. *Pharmaceut* 14:660–672
- Ceramella J, Groo A, Iacopetta D, S'eguy S. et al (2021) A winning strategy to improve the anticancer properties of Cisplatin and Quercetin based on the nanoemulsions formulation. *J Drug Deliv Sci Technol* 66:102907
- Cha D, Moon E, Kim Y, Cha H, Lee Y (2009) Essential oil of *artemisia capillaris* induces apoptosis in KB cells via mitochondrial stress and caspase activation mediated by MAPK-stimulated signaling pathway. *J Food Sci* 74:T75–T81
- Chen W, Liu Y, Li M, Mao J et al (2015) Anti-tumor effect of α -pinene on human hepatoma cell lines through inducing G2/M cell cycle arrest. *J Pharmacol Sci* 127(3):332–338
- Cheok C (2012) Protecting normal cells from the cytotoxicity of chemotherapy. *Cell Cycle* 11:2227–2232
- Deng Y, Zhao P, Zhou L, Xiang D et al (2020) Epidemiological trends of tracheal, bronchus, and lung cancer at the global, regional, and national levels: a population-based study. *J Hematol Oncol* 13:98–113
- Edris A (2021) Development and characterization of ethanol-free spearmint essential oil nanoemulsion for food applications using the low energy technique. *Gras y Aceit* 72:e431–e431
- Efferth T, Oesch F (2020) Anti-inflammatory and anti-cancer activities of frankincense: Targets, treatments and toxicities. *Semin Cancer Biol* 80:39–57
- Falleh H, Ben Jemaa M, Neves M, Mitsutoshi H et al (2021) Peppermint and Myrtle nanoemulsions: Formulation, stability, and antimicrobial activity. *Nanomed* 152:112377
- Flores-Romero H, Hohorst L, John M et al (2022) BCL-2-family protein tBID can act as a BAX-like effector of apoptosis. *EMBO J* 41:e108690
- Garti N, Yaghmur A, Leser M, Clement V, Watzke H (2001) Improved oil solubilization in oil/water food grade microemulsions in the presence of polyols and ethanol. *J Agric Food Chem* 49:2552–2562
- Gasparian E, Chernyak V, Dolgikh A, Yagolovich V, Popova N et al (2009) Generation of new TRAIL mutants DR5-A and DR5-B with improved selectivity to death receptor 5. *Apoptosis Int J Program Cell Death* 14:778–787
- Hakkim L, Bakshi A, Khan S, Nasef M et al (2020) Frankincense essential oil suppresses melanoma cancer through down regulation of Bcl-2/Bax cascade signaling and ameliorates hepatotoxicity via phase I and II drug metabolizing enzymes. *Oncotarget* 11(23):2259–2261
- Hoy H, Lynch T, Beck M (2019) Surgical treatment of lung cancer. *Crit Care Nurs Clin North Am* 31(3):303–313
- Huang M, Lu J, Ding J (2021) Natural products in cancer therapy: Past, present and future. *Nat Prod Bioprospect* 11:5–13
- Kannappan R, Ravindran J, Prasad S, Sung B et al (2010) Gamma-tocotrienol promotes TRAIL-induced apoptosis through reactive oxygen species/extracellular signal-regulated kinase/p53-mediated upregulation of death receptors. *Mol Canc Ther* 9:2196–2207
- Katragunta K, Siva B, Kondepudi N, Vadaparthy R et al (2019) Estimation of boswellic acids in herbal formulations containing *Boswellia serrata* extract and comprehensive characterization of secondary metabolites using UPLC-Q-ToF-MS. *J Pharm Anal* 9:414–422
- Khalifa J, Lerouge D, Le Pêchoux C, Pourel N et al (2021) Radiotherapy for primary lung cancer Radiothérapie des cancers primitifs du poumon. *Cancer/radiothérapie* 26:231–243
- Kieliszek M, Edris A, Kot A, Piwowarek K (2020) Biological activity of some aromatic plants and their metabolites, with an emphasis on health-promoting properties. *Molecules* 25:2478–2497
- Kumar A, Dev K, Sourirajan A (2021) Essential oils of *Rosmarinus officinalis* L., *Cymbopogon citratus* (DC.) Stapf., and the phyto-compounds, delta-carene and alpha-pinene mediate cell cycle arrest at G2/M transition in budding yeast *Saccharomyces cerevisiae*. *South Afr J Bot* 141:296–305
- Li A, Flores K, Canavan M, Boffa D et al (2022) Adjuvant chemotherapy for T4 non-small cell lung cancer with additional ipsilateral lung nodules. *Ann Thorac Surg* 113:421–428
- Lu M, Xia L, Hua H, Jing Y (2008) Acetyl-keto-beta-boswellic acid induces apoptosis through a death receptor 5-mediated pathway in prostate cancer cells. *Cancer Res* 68:1180–1186
- Lv M, Shao S, Zhang Q, Zhuang X, Qiao T (2020) Acetyl-11-Keto- β -boswellic acid exerts the anti-cancer effects via cell cycle arrest, apoptosis induction and autophagy suppression in non-small cell lung cancer cells. *Onco Targets Ther* 13:733–744
- Mahalingam D, Szegezdi E, Keane M, de Jong S, Samali A (2009) TRAIL receptor signalling and modulation: Are we on the right TRAIL? *Cancer Treat Rev* 35:280–288
- Mertens M, Buettnera A, Kirchoff E (2009) The volatile constituents of frankincense: a review. *Flav Fragr* 24:279–300
- Mikhaeil R, Maatooq T, Badria A, Amer M (2003) Chemistry and immunomodulatory activity of frankincense oil. *Z Naturforsch C J Biosci* 58:230–238
- Nazim U, Yin H, Park S (2020) Downregulation of c-FLIP and upregulation of DR-5 by cantharidin sensitizes TRAIL-mediated apoptosis in prostate cancer cells via autophagy flux. *Int J Mol Med* 6:280–288
- Nguyen T, Kumar V, Ponnusamy V, Mai T et al (2021) Phytochemicals intended for anticancer effects at preclinical levels to clinical practice: Assessment of formulations at nanoscale for non-small cell lung cancer (NSCLC) therapy. *Process Biochem* 104:55–75

- Omara T, Kiprop A (2020) Medicinal plants used in traditional management of cancer in Uganda: A review of ethnobotanical surveys. *Phytochem Anticancer Stud* 9:3529081
- Park J, Choi S, Yoo H, Kwon K (2013) Nutlin-3, a small-molecule MDM2 inhibitor, sensitizes Caki cells to TRAIL-induced apoptosis through p53-mediated PUMA upregulation and ROS-mediated DR5 upregulation. *Anticancer Drug* 24:260–269
- Passiglia F, Bertaglia V, Reale M, Delcuratolo M et al (2021) Major breakthroughs in lung cancer adjuvant treatment: Looking beyond the horizon. *Cancer Treat Rev* 101:102308
- Refaat A, Abd-Rabou A, Reda A (2014) TRAIL combinations: The new 'trail' for cancer therapy (Review). *Oncol Lett* 7:1327–1332
- Reis D, Jones T (2018) Frankincense essential oil as a supportive therapy for cancer-related fatigue: A case study. *Holist Nurs Pract* 32:140–142
- Ren P, Ren X, Cheng L, Xu L (2018) Frankincense, pine needle and geranium essential oils suppress tumor progression through the regulation of the AMPK/mTOR pathway in breast cancer. *Oncol Rep* 39:129–137
- Rodriguez-Canales J, Parra-Cuentas E, Wistuba I (2016) Diagnosis and molecular classification of lung cancer. *Cancer Treat Res* 170:25–46
- Siddiqui A, Shah Z, Jahan R, Othman I, Kumari Y (2021) Mechanistic role of boswellic acids in Alzheimer's disease: Emphasis on anti-inflammatory properties. *Biomed Pharmacother* 144:112250
- Siegel R, Miller K, Fuchs H, Jemal A (2021) Cancer Statistics. *CA Cancer J Clin* 71:7–33
- Singh J, Luqman S, Meena A (2021) Emerging role of phytochemicals in targeting predictive, prognostic, and diagnostic biomarkers of lung cancer. *Food Chem Toxicol* 144:111592
- Sœur J, Marrot L, Perez P et al (2011) Selective cytotoxicity of *Aniba rosaeodora* essential oil towards epidermoid cancer cells through induction of apoptosis. *Mutat Res* 718:24–32
- Suhail M, Wu W, Cao A, Mondalek G et al (2011) *Boswellia sacra* essential oil induces tumor cell-specific apoptosis and suppresses tumor aggressiveness in cultured human breast cancer cells. *BMC Complement Altern Med* 11:129–142
- Suster D, Mino-Kenudson M (2020) Molecular pathology of primary non-small cell lung cancer. *Arch Med Res* 51(8):784–798
- Tan A, Tan S, Zhou S, Peters S et al (2022) Efficacy of targeted therapies for oncogene-driven lung cancer in early single-arm versus late phase randomized clinical trials: A comparative analysis. *Cancer Treat Rev* 104:102354
- Titan A, He H, Lui N, Liou D et al (2020) The influence of hormone replacement therapy on lung cancer incidence and mortality. *J Thoracic Cardiovas Surg* 159:1546–1556
- Tokuoka Y, Uchiyama H, Abe M (1993) Phase Diagrams of Surfactant/water/synthetic Perfume Ternary Systems. *Colloid Polym Sci* 272:317–323
- van Meerloo J, Kaspers G, Cloos J (2011) Cell sensitivity assays: the MTT assay. *Methods Mol Biol* 731:237–245
- Van Vuuren F, Kamatou G, Viljoen A (2010) Volatile composition and antimicrobial activity of twenty commercial frankincense essential oil samples. *South Afr J Botan* 76:686–769
- Wang R, Shang J, Zhao X (2021) Alpha-pinene induces apoptosis through oxidative stress and PI3K/AKT/NF- κ B Signalling Pathway in MDA-MB-231 human breast cancer cells. *Int J Pharmacol* 17:391–399
- Wilson R, Li Y, Yang G, Zhao C (2022) Nanoemulsions for drug delivery. *Particuology* 64:85–97
- Woolley L, Suhail M, Smith L, Boren E, Taylor C et al (2012) Chemical differentiation of *Boswellia sacra* and *Boswellia carterii* essential oils by gas chromatography and chiral gas chromatography-mass spectrometry. *J Chromatogr A* 1261:158–163
- Xue T, Zhao X, Zhao K, Lu Y, Yao J et al (2022) Immunotherapy for lung cancer: Focusing on chimeric antigen receptor (CAR)-T cell therapy. *Curr Probl Cancer* 23:100791
- Yaman C, Sari Y, Atmaca S, Eroglu Z et al (2021) Chemical composition and biological effects of essential oils from some aromatic and medicinal plants. *Nat Prod J* 11(5):699–706
- Yoo Y, Lee J, Jung E, Park M et al (2020) Data on cytotoxicity of plant essential oils in A549 and Detroit 551 cells. *Data Brief* 32:106186
- Zhang Z, Guo S, Liu X, Gao X (2015) Synergistic antitumor effect of α -pinene and β -pinene with paclitaxel against non-small-cell lung carcinoma (NSCLC). *Drug Res (stuttg)* 65:214–218
- Zhao Y, Dai D, Lu C, Chen L et al (2013) Epirubicin loaded with propylene glycol liposomes significantly overcomes multi-drug resistance in breast cancer. *Cancer Lett* 330:74–83
- Zhao Y, Chen R, Wang Y, Yang Y (2018) α -Pinene inhibits human prostate cancer growth in a mouse xenograft model. *Chemother* 63:1–7

Publisher's Note

Springer Nature remains neutral with regard to jurisdictional claims in published maps and institutional affiliations.